

**COMMENTARY**

# Mammalian muscle fibers may be simple as well as slow

 John M. Squire<sup>1,2</sup>  and Pradeep K. Luther<sup>3</sup> 

One of the thrills of science is when a discovery made long ago, and nearly forgotten, gets picked up when viewing it from a new perspective and receives a whole new lease on life. The lattice arrangement of myosin filaments in vertebrate striated muscles is a case in point (see [Ma et al.](#) in this issue of the *Journal of General Physiology*). In the vertebrate muscle sarcomere, the myosin filaments in the A-band are arranged in a hexagonal lattice. In their classic study, [Huxley and Brown \(1967\)](#) examined frog (amphibian) sartorius muscle by x-ray diffraction and found that the arrangement was one in which immediately neighboring filaments did not have the same rotations around their long axes, but the next-nearest ones often did ([Fig. 1 c](#)). They called this a superlattice arrangement. The contents of the superlattice were discovered by [Luther and Squire \(1980\)](#) by means of electron microscopy of thin transverse sections of frog muscle. They showed that the myosin filaments, which have a threefold rotational symmetry ([Squire, 1972](#)), had one of two orientations on the lattice, 0 or 60°. They showed that, to generate a superlattice arrangement, filaments can be placed on a lattice with rotations determined by two simple rules (the “no-three-alike” rules; [Fig. 1, d and f](#)), which generate a superlattice of limited extent. However, further research by us ([Luther et al., 1981](#)) and [Pepe \(1975\)](#) revealed that vertebrate striated muscles do not always have a superlattice arrangement of myosin filaments. In particular, it was found that, in the muscles of bony fish, all myosin filaments have the same rotation around their long axes ([Fig. 1b](#)). This is called a simple lattice. [Ma et al. \(2019\)](#) have shown for the first time that a simple lattice structure occurs in some mammalian muscles as well.

Vertebrate skeletal muscle fibers and myofibrils have a characteristic cross-striated appearance such that each striation corresponds to the sarcomere-repeating unit of the muscle. As shown in the classic studies of [Huxley and Hanson \(1954\)](#) and [Huxley and Niedergerke \(1954\)](#), sarcomeres have a regular arrangement of overlapping myosin and actin filaments ([Fig. 1 a](#);

see also [Fig. 4 a](#)). The myosin filaments are bipolar; their component myosin molecules, with their globular ATPase heads projecting outward, point in opposite directions in the two halves of the central A-band. At their halfway point, they are cross-linked at the M-band by proteins such as myomesin and M-protein ([Lange et al., 2019](#)). Both halves of the myosin filaments contain myosin-binding protein C (MyBP-C; C-protein) along part of their length ([Tonino et al., 2019](#)). Actin filaments are polar, and they point in opposite directions at each end of the sarcomere. The polarity changes across the Z-line (Z-band; [Fig. 1](#)), which cross-links the actin filaments primarily through the protein  $\alpha$ -actinin ([Burgoyne et al., 2019](#)). Actin filaments carry the regulatory proteins tropomyosin and troponin ([Paul et al., 2017](#)). Another major protein component of the sarcomere is the enormous molecule titin ([Ottenheijm and Granzier, 2010](#); [Knupp et al., 2002](#); [Azad et al., 2019](#); [Tonino et al., 2019](#)). Titin binds to myosin filaments from the M-band to the filament tip and then extends through the I-band to the Z-line.

This filament arrangement is characteristic of all vertebrate striated muscles—both skeletal and cardiac. However, some muscles contract quickly at the expense of fatiguing rapidly, while others are much slower but can maintain tension for longer. Some fibers have intermediate properties. Many muscles are a mixture of fast, slow, and intermediate fiber types; the proportion of different fibers is related to the physiological role of that particular muscle. The different behaviors of specific fiber types are due, in part, to the presence of different isoforms of the same sarcomeric proteins (e.g., myosin, actin, titin, MyBP-C, tropomyosin, and troponin; [Bandman, 1992](#)). Some of their effects can be rather subtle and may only manifest themselves when assessing the detailed physiological characteristics of the fibers. However, other differences are much more obvious. For example, different isoforms can alter the Z-line and M-band structures in ways that can be seen in electron micrographs ([Luther, 2009](#); [Pask et al., 1994](#)). Another major effect is on the way that myosin

<sup>1</sup>Muscle Contraction Group, School of Physiology, Pharmacology and Neuroscience, University of Bristol, Bristol, UK; <sup>2</sup>Computational and Systems Medicine, Faculty of Medicine, Imperial College London, London, UK; <sup>3</sup>Molecular Medicine Section, National Heart and Lung Institute, Imperial College London, London, UK.

Correspondence to John M. Squire: [j.m.squire@bristol.ac.uk](mailto:j.m.squire@bristol.ac.uk); Pradeep K. Luther: [p.luther@imperial.ac.uk](mailto:p.luther@imperial.ac.uk).

© 2019 Squire and Luther. This article is distributed under the terms of an Attribution–Noncommercial–Share Alike–No Mirror Sites license for the first six months after the publication date (see <http://www.rupress.org/terms/>). After six months it is available under a Creative Commons License (Attribution–Noncommercial–Share Alike 4.0 International license, as described at <https://creativecommons.org/licenses/by-nc-sa/4.0/>).

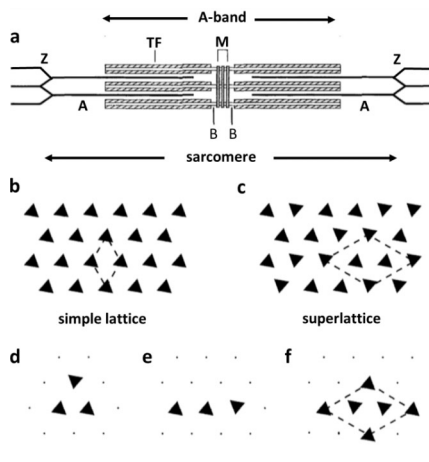


**Figure 1. The structural arrangement of striated muscle sarcomeres.** (a) Schematic diagram of a vertebrate striated muscle sarcomere with the thick myosin filaments (TF) forming the A-band and overlapping actin filaments (A), which extend to the Z-line (Z). Myosin filaments are cross-linked at the M-band (M), on each side of which are the bare regions (B), where the myosin filament backbone appears triangular (see also Fig. 4 a). The I-band extends from the A-band edges to the Z-line. (b and c) The appearance in electron micrographs of cross sections through the bare regions in panel a, for the simple lattice (b) and the superlattice (c). (d-f) Illustrations of the no-three-alike rules, and a superlattice unit cell where the no-three-alike rules have been applied (f). Adapted from [Luther et al. \(1996\)](#), with permission.

filaments are arranged in the muscle A-band, which is the topic of the paper by [Ma et al. \(2019\)](#) in this issue.

#### Visualizing the myosin filament superlattice

[Huxley \(1963\)](#) showed that the antiparallel configuration of myosin molecules in myosin filaments leaves a region free of heads  $\sim 160$  nm long in the middle. The M-band is located in the middle of this zone, which Huxley called the bare zone. The triangular shape of the myosin filament backbone (see Fig. 1, b and c) is most evident in the two spaces between the M-band and the position where the myosin heads start to project from the filament surface. [Luther and Squire \(1980\)](#) termed these the bare regions (Figs. 1 a and 4 a). Surprisingly, they found that the distribution of the triangular profiles across the myofibril was not regular in the bare regions and that the orientations instead obeyed the two no-three-alike rules mentioned earlier. Specifically, three myosin filaments in a row do not usually have the same rotation, and three myosin filaments at the corners of a triangle do not usually have the same rotation. As discussed later, these two rules cannot be applied perfectly across the myofibril. But if the rules are optimized, a statistical myosin filament superlattice can be generated (Fig. 1 c) in which the filaments at the corners of the unit cell tend to have the same rotation and the two filaments in the middle of the unit cell can have either of the two rotations (0 or 60°). Such superlattices do not tend to occur over a large number of unit cells; the wider distribution of filament rotations is rather irregular.

#### Some A-bands are simple

As noted above, a surprising discovery by [Pepe \(1975\)](#), [Luther and Squire \(1980\)](#), and [Harford and Squire \(1986\)](#) was that not

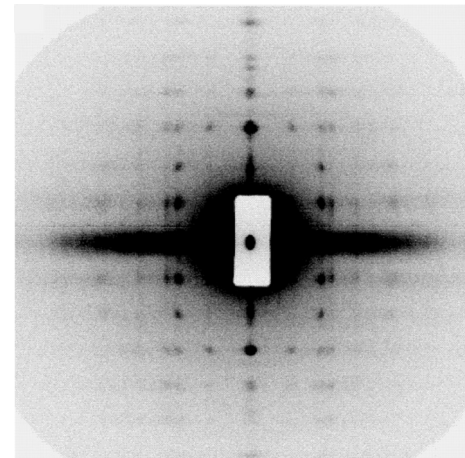


**Figure 2. An example of a beautifully ordered low-angle x-ray diffraction pattern from a bony fish muscle.** The axis of the muscle fiber is vertical. Horizontal rows of spots (layer lines) come mostly from the myosin heads on the myosin filaments. They index on an axial repeat of 42.9 nm. Rows of spots in the vertical direction (row lines) provide information about how the myosin filaments are organized in 3-D in the hexagonal A-band lattice. This is the typical pattern of a well-ordered simple lattice muscle. Adapted from [Hudson et al. \(1997\)](#), with permission.

all vertebrate striated muscles have a superlattice in their A-bands. These studies on bony fish muscles found that all the triangular profiles of myosin filaments across an A-band in a myofibril had exactly the same rotations (Fig. 1 b). In other words, they contain a simple myosin filament lattice and not a superlattice. The simple lattice makes the whole of the A-band much more regular, and x-ray diffraction patterns from bony fish muscles, in particular, are beautifully sampled to give almost crystalline fiber diffraction patterns (Fig. 2). The presence of a highly ordered simple lattice makes it much easier to carry out ultrastructural studies. Indeed, considerable insight into muscle architecture and function has come from studying these regular muscles (e.g., [Luther et al., 1981](#); [Hudson et al., 1997](#); [Eakins et al., 2019](#); [Knupp et al., 2019](#)).

#### Evolution of muscle types

Because some muscles have a simple lattice and some a superlattice, it was of interest to study sarcomeres throughout the animal kingdom to discover how these two structures evolved. The results of such a systematic study, performed by [Luther et al. \(1996\)](#), are illustrated in Fig. 3. To study the A-band lattice of every species is clearly an impossibility, so as many representative examples as possible were studied in each order of the craniates. In addition, studies in the literature were scrutinized to see if they provided evidence of either lattice type. The surprising discovery was that both super- and simple lattice arrangements were present in fast white and slow red shark muscles, respectively. The general conclusion of the study was that the disordered superlattice arrangement came first, as seen in hagfishes and lampreys, and that the simple lattice emerged in the elasmobranchs (sharks and rays), in which both lattice types are seen in different muscles, and chimaera, which is superlattice. More recent vertebrates, the osteichthyes, can

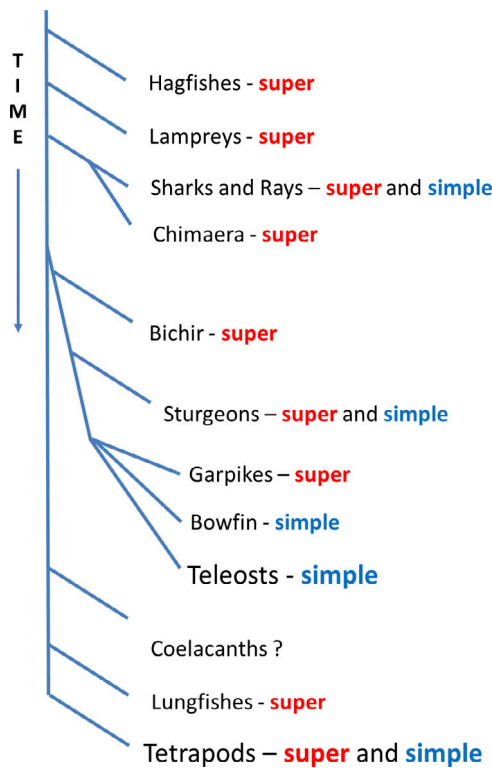


**Figure 3. A simple evolutionary tree for the craniates showing where simple lattices and superlattices have been found.** Data from Luther et al. (1996), Luther and Squire (2014), and Ma et al. (2019). Particularly large families are the teleosts, where all muscles studied so far have simple lattices, and the tetrapods (mammals, amphibians, reptiles, and birds), which until now have generally shown superlattice structures. The work of Ma et al. (2019) has now found the simple lattice structure in rat SOL muscles, which consist predominantly of slow fibers.

show either lattice type, except the teleosts (bony fish), in which the simple lattice seems to always be present. In the case of later vertebrates (lungfishes, tetrapods), it was thought that the superlattice had prevailed. However, the new results of Ma et al. (2019) throw a new light on what is going on, at least in mammalian muscles, which seem to follow the pattern found in shark muscle.

#### The new observations

Most muscles are a mixture of fiber types, but there are one or two mammalian muscles that are predominantly of one type. For example, in the rat the extensor digitorum longus (EDL) muscle consists almost wholly of fast fibers (types IIA, IIB, and IID/X), whereas the soleus (SOL) is 85–95% slow (type I) and only 5–15% fast IIA. Ma et al. (2019) performed electron microscopy of thin transverse sections through the bare regions of these muscles, as well as low-angle x-ray diffraction. They found that the fast EDL muscle appeared to show the superlattice structure, although not very highly developed. Much clearer was that the slow SOL muscle showed strong evidence of a simple lattice. The bare region transverse sections showed triangular filament profiles with similar rotations (Fig. 1 b), and the x-ray diffraction patterns showed similar layer-line sampling to that in Fig. 2. Assuming that the ratio of slow to fast fibers in SOL is roughly 9:1

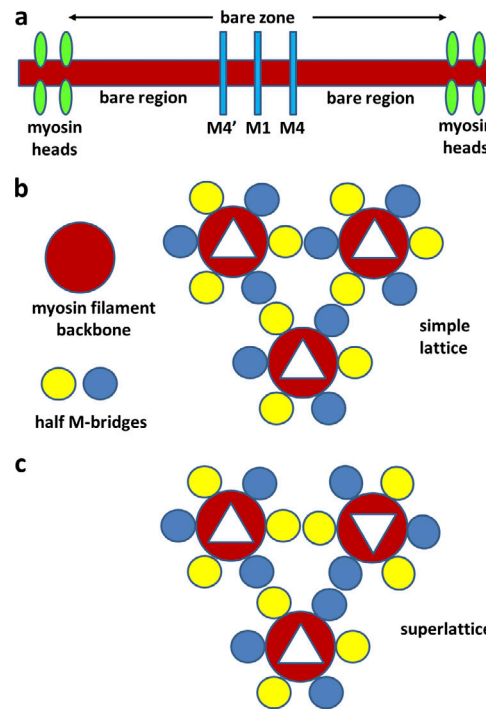


**Figure 4. Comparison of simple lattice and superlattice arrangements in the M-band.** (a) Illustration of the myosin filament bare zone (the whole length between the first left and right myosin head positions) and the M-lines (M4', M1, and M4), which form part of the M-band. Some fiber types have more lines (M6 and M6') equally spaced outside the other lines. The bare regions lie between the M-band and the level of the first myosin head. (b and c) Schematic illustrations of the possible origins of the simple lattice and superlattice packing interactions at the M-band. The bare zone structure in panel a has the symmetry of the dihedral point group 32 (Luther et al., 1981; Al-Khayat et al., 2010). This means that it has threefold rotational symmetry around the filament long axis and three twofold rotation axes at right angles to the threefold axis and in the plane of M1. The myosin filament makes bridges in the M-band to all six surrounding myosin filaments in the hexagonal lattice, three of which must have the opposite polarity to the other three (i.e., rotated by 180° around a twofold axis). These two possibilities are shown by yellow and blue circles. The yellow and blue half-bridges represent the same molecular structure, but rotated around a twofold axis by 180°. (b) Unlike interactions automatically generate a simple lattice, as indicated by the white triangles. (c) On the other hand, if like-with-like interactions are preferred, then two out of three interactions can be satisfied for three filaments on a triangle, but the rotation of the third filament will always be ambivalent (at least one of the interactions must be an unlike interaction). Optimizing the like interactions inevitably produces a statistical superlattice. For details, see text.

and that all fast fibers have a superlattice structure, the effect on the x-ray diffraction pattern would be minimal. The intensity of peaks in x-ray diffraction patterns is proportional to the square of the mass of the diffracting material, so 9:1 fiber content would give intensities in the ratio 81:1, assuming the fibers in the two fiber types have roughly the same diameter. The simple lattice pattern would clearly dominate, and the diffraction from any minor superlattice component would be smothered.

#### Do all slow mammalian fibers have a simple lattice?

A prior study of mouse diaphragms, which are thought to contain ~98% fast-twitch, fatigue-resistant fibers (type IIA), showed

x-ray diffraction evidence of a simple lattice (Iwamoto et al., 2003). Ma et al. (2019) suggest that maybe it is not just slow fibers that are simple, but fatigue-resistant fibers are, too. Luther et al. (1996) showed that sharks and rays have fast white fibers with a superlattice and slow red fibers with a simple lattice, revealing a potential trend in some animals. Perhaps it is also a common property of mammals that slow-fatigue fibers have a simple lattice, and other fibers have a superlattice. If so, the correlation is not perfect across the craniates because teleosts have slow red and fast white fibers, all of which appear to have simple lattice A-bands.

### Why would simple and superlattice A-bands be functionally different?

Evolutionary changes usually confer an advantage; otherwise, they would presumably not occur. So why would a simple lattice evolve from a superlattice for some animals (Fig. 3)? Of course, it is possible that there is no advantage and that it was a neutral evolutionary change. However, it is of interest to consider what functional changes the different rotations would make. Remembering that each actin filament is surrounded by three myosin filaments in the vertebrate A-band lattice, the different filament rotations will produce different myosin head arrangements around the actin filament. As detailed in Fig. 5 of Luther et al. (1996), the superlattice tends to spread the myosin heads along the actin filament so that, in principle, head interactions can occur at any actin position and the heads on different myosin filaments are not competing for the same actin binding sites. The simple lattice, on the other hand, has the effect of placing six myosin heads at the same axial level around an actin filament, leaving other parts of the actin filament with few heads available. At first sight, this seems more of a disadvantage than an advantage. One effect might be to reduce the tension produced by the simple lattice muscles, perhaps to reduce the ATP turnover rate (Luther and Squire, 2014). In teleosts, where simple lattices dominate, the bulky white body muscle defines the shape and streamline of the fish, and the small strip of red fibers along the lateral line provides most of the force for slow swimming. The white fibers are generally not used for this swimming, but are available for rapid escape or predatory responses (Rome et al., 1988). Perhaps the simple lattice of the white fibers in the bulk of the fish reduces ATP usage. Simple lattice muscles do appear to produce lower isometric tensions than superlattice muscles, but the different protein isoforms in the different muscles make it difficult to determine if the lower tension is a lattice effect or something else. If it turns out that mammalian slow fibers often have a simple lattice, then elucidating the advantage that this gives will be an important future target.

### Which molecular structure defines the A-band lattice type?

Our final comment is about the structure in the A-band that defines the two lattice types. Fig. 4 illustrates what might be going on. We know from previous studies that the bare-zone regions of vertebrate striated muscle myosin filaments have the symmetry of the dihedral point group 32 (Luther et al., 1981; Al-Khayat et al., 2010). This means that, in addition to the

threefold rotational symmetry around the filament long axis, there are three twofold rotation axes at the level of M1 in the M-band (Fig. 4 a) perpendicular to the threefold axis and spaced at 120° intervals around the threefold axis. Because myosin filaments make M-bridge connections with each of their six surrounding myosin filament neighbors in the M-band, the M-bridge interactions must be of two types, as indicated by different colors (blue and yellow) in Fig. 4 b. Each set has three bridges spaced 120° apart around the long axis of the filament. The two types represent the same molecular structure, but one set would be rotated by 180° around a twofold axis to give the other. Fig. 4 b shows that, if the interaction at the M-band is always between M-bridges of opposite polarity (blue and yellow circles), then a regular simple lattice structure is always generated. On the other hand, problems prevail if like interactions are preferred (Fig. 4 c). Roughly two out of three M-bridge interactions can be made between like partners, but inevitably some unlike interactions will be made as well. If, while building up an A-band, the like interactions are optimized, then a statistical superlattice is automatically generated. This is an example of geometrical frustration and is a well-known phenomenon in solid-state physics (Wannier, 1950). Details of which M-band proteins are involved in these interactions have yet to be determined, although structures at the level of M4 have been suggested since the M4 bridges always seem to be present in different M-bands, but the M1 and M6 densities vary. Obtaining good ultrastructural data on the M-band is an urgent priority.

### Acknowledgments

Henk L. Granzier served as editor.

The author declares no competing financial interests.

### References

- Al-Khayat, H.A., R.W. Kensler, E.P. Morris, and J.M. Squire. 2010. Three-dimensional structure of the M-region (bare zone) of vertebrate striated muscle Myosin filaments by single particle analysis. *J. Mol. Biol.* 403:763–776. <https://doi.org/10.1016/j.jmb.2010.09.025>
- Azad, A., G. Poloni, N. Sontayananon, H. Jiang, and K. Gehmlich. 2019. The giant titin: how to evaluate its role in cardiomyopathies. *J. Muscle Res. Cell Motil.* 40:159–167. <https://doi.org/10.1007/s10974-019-09518-w>
- Bandman, E. 1992. Contractile protein isoforms in muscle development. *Dev. Biol.* 154:273–283. [https://doi.org/10.1016/0012-1606\(92\)90067-Q](https://doi.org/10.1016/0012-1606(92)90067-Q)
- Burgoyne, T., J.M. Heumann, E.P. Morris, C. Knupp, J. Liu, M.K. Reedy, K.A. Taylor, K. Wang, and P.K. Luther. 2019. Three-dimensional structure of the basketweave Z-band in midshipman fish sonic muscle. *Proc. Natl. Acad. Sci. USA.* 116:15534–15539. <https://doi.org/10.1073/pnas.1902235116>
- Eakins, F., C. Knupp, and J.M. Squire. 2019. Monitoring the myosin cross-bridge cycle in contracting muscle: steps towards 'Muscle-the Movie'. *J. Muscle Res. Cell Motil.* 40:77–91. <https://doi.org/10.1007/s10974-019-09543-9>
- Harford, J., and J.M. Squire. 1986. Crystalline myosin cross-bridge array in relaxed bony fish muscle. *Biophys. J.* 50:145–155. [https://doi.org/10.1016/S0006-3495\(86\)83447-6](https://doi.org/10.1016/S0006-3495(86)83447-6)
- Hudson, L., J.J. Harford, R.C. Denny, and J.M. Squire. 1997. Myosin head configuration in relaxed fish muscle: resting myosin heads must swing axially by up to 150 Å or turn upside down to reach rigor. *J. Mol. Biol.* 273:440–455. <https://doi.org/10.1006/jmbi.1997.1321>
- Huxley, H.E. 1963. Electron microscope studies on the structure of natural and synthetic protein filaments from striated muscle. *J. Mol. Biol.* 7: 281–308. [https://doi.org/10.1016/S0022-2836\(63\)80008-X](https://doi.org/10.1016/S0022-2836(63)80008-X)

- Huxley, H.E., and W. Brown. 1967. The low-angle X-ray diagram of vertebrate striated muscle and its behaviour during contraction and rigor. *J. Mol. Biol.* 30:383–434. [https://doi.org/10.1016/S0022-2836\(67\)80046-9](https://doi.org/10.1016/S0022-2836(67)80046-9)
- Huxley, H., and J. Hanson. 1954. Changes in the cross-striations of muscle during contraction and stretch and their structural interpretation. *Nature*. 173:973–976. <https://doi.org/10.1038/173973a0>
- Huxley, A.F., and R. Niedergerke. 1954. Structural changes in muscle during contraction; interference microscopy of living muscle fibres. *Nature*. 173:971–973. <https://doi.org/10.1038/173971a0>
- Iwamoto, H., J. Wakayama, T. Fujisawa, and N. Yagi. 2003. Static and dynamic X-ray diffraction recordings from living mammalian and amphibian skeletal muscles. *Biophys. J.* 85:2492–2506. [https://doi.org/10.1016/S0006-3495\(03\)74672-4](https://doi.org/10.1016/S0006-3495(03)74672-4)
- Knupp, C., P.K. Luther, and J.M. Squire. 2002. Titin organisation and the 3D architecture of the vertebrate striated muscle I-Band. *J. Mol. Biol.* 322: 731–739. [https://doi.org/10.1016/S0022-2836\(02\)00819-7](https://doi.org/10.1016/S0022-2836(02)00819-7)
- Knupp, C., E. Morris, and J.M. Squire. 2019. The interacting head motif structure does not explain the x-ray diffraction patterns in relaxed vertebrate (bony fish) skeletal muscle and insect (*Lethocerus*) flight muscle. *Biology (Basel)*. 8:E67. <https://doi.org/10.3390/biology8030067>
- Lange, S., N. Pinotsis, I. Agarkova, and E. Ehler. 2019. The M-band: The underestimated part of the sarcomere. *Biochim. Biophys. Acta Mol Cell Res.* In press. <https://doi.org/10.1016/j.bbamcr.2019.02.003>
- Luther, P.K., and J.M. Squire. 1980. Three-dimensional structure of the vertebrate muscle A-band. II. The myosin filament superlattice. *J. Mol. Biol.* 141:409–439. [https://doi.org/10.1016/0022-2836\(80\)90254-5](https://doi.org/10.1016/0022-2836(80)90254-5)
- Luther, P.K., P.M. Munro, and J.M. Squire. 1981. Three-dimensional structure of the vertebrate muscle A-band. III. M-region structure and myosin filament symmetry. *J. Mol. Biol.* 151:703–730. [https://doi.org/10.1016/0022-2836\(81\)90430-7](https://doi.org/10.1016/0022-2836(81)90430-7)
- Luther, P.K., J.M. Squire, and P.L. Forey. 1996. Evolution of myosin filament arrangements in vertebrate skeletal muscle. *J. Morphol.* 229:325–335. [https://doi.org/10.1002/\(SICI\)1097-4687\(199609\)229:3<325::AID-JMOR7>3.0.CO;2-X](https://doi.org/10.1002/(SICI)1097-4687(199609)229:3<325::AID-JMOR7>3.0.CO;2-X)
- Luther, P.K. 2009. The vertebrate muscle Z-disc: sarcomere anchor for structure and signalling. *J. Muscle Res. Cell Motil.* 30:171–185. <https://doi.org/10.1007/s10974-009-9189-6>
- Luther, P.K., and J.M. Squire. 2014. The intriguing dual lattices of the myosin filaments in vertebrate striated muscles: evolution and advantage. *Biology (Basel)*. 3:846–865.
- Ma, W., K.H. Lee, S. Yang, T.C. Irving, and R. Craig. 2019. Lattice arrangement of myosin filaments correlates with fiber type in rat skeletal muscle. *J. Gen. Physiol.* <https://doi.org/10.1085/jgp.201912460>
- Ottenheijm, C.A., and H. Granzier. 2010. Role of titin in skeletal muscle function and disease. *Adv. Exp. Med. Biol.* 682:105–122. [https://doi.org/10.1007/978-1-4419-6366-6\\_6](https://doi.org/10.1007/978-1-4419-6366-6_6)
- Pask, H.T., K.L. Jones, P.K. Luther, and J.M. Squire. 1994. M-band Structure, M-bridge interactions and contraction speed in vertebrate cardiac muscles. *J. Muscle Res. Cell Motil.* 15:633–645. <https://doi.org/10.1007/BF00121071>
- Paul, D.M., J.M. Squire, and E.P. Morris. 2017. Relaxed and active thin filament structures: a new structural basis for the regulatory mechanism. *J. Struct. Biol.* 197:365–371. <https://doi.org/10.1016/j.jsb.2017.01.004>
- Pepe, F.A. 1975. Structure of muscle filaments from immunohistochemical and ultrastructural studies. *J. Histochem. Cytochem.* 23:543–562. <https://doi.org/10.1177/23.7.1095653>
- Rome, L.C., R.P. Funke, R.M. Alexander, G. Lutz, H. Aldridge, F. Scott, and M. Freedman. 1988. Why animals have different muscle fibre types. *Nature*. 335:824–827. <https://doi.org/10.1038/335824a0>
- Squire, J.M. 1972. General model of myosin filament structure II: myosin filaments and crossbridge interactions in vertebrate striated and insect flight muscles. *J. Mol. Biol.* 72:125–138. [https://doi.org/10.1016/0022-2836\(72\)90074-5](https://doi.org/10.1016/0022-2836(72)90074-5)
- Tonino, P., B. Kiss, J. Gohlke, J.E. Smith III, and H. Granzier. 2019. Fine mapping titin's C-zone: Matching cardiac myosin-binding protein C stripes with titin's super-repeats. *J. Mol. Cell. Cardiol.* 133:47–56. <https://doi.org/10.1016/j.yjmcc.2019.05.026>
- Wannier, G.H. 1950. Antiferromagnetism. The triangular ising net. *Phys. Rev.* 79:357–364. <https://doi.org/10.1103/PhysRev.79.357>